Supporting Information

Sb^{3+}-doped 0D Cs_3GdCl_6 microcrystals with a near-unity photoluminescence quantum yield and high thermal quenching resistance for light-emitting application

Xiantian Liang,[‡a,b] Wei Zhang,[‡a,c] Yitong Shi,[a,b] Wen Zhang,[a] Hongyi Yang,[a] Ping Huang,[a,b] Lingyun Li,[c] Qi Zhang,[c] Wei Zheng*[a,b] and Xueyuan Chen[a,b]

a. CAS Key Laboratory of Design and Assembly of Functional Nanostructures, Fujian Key Laboratory of Nanomaterials, and State Key Laboratory of Structural Chemistry, Fujian Institute of Research on the Structure of Matter, Chinese Academy of Sciences, Fuzhou, Fujian 350002, China.
E-mail: zhengwei@fjirsm.ac.cn

b. College of Physics and Energy, Fujian Normal University, Fuzhou, Fujian 350117, China.

c. Key Laboratory of Advanced Materials Technologies and International (Hongkong, Macao and Taiwan) Joint Laboratory on Advanced Materials Technologies, College of Materials Science and Engineering, Fuzhou University, Fuzhou, Fujian 350108, China.

‡ Xiantian Liang and Wei Zhang contributed equally to this article.

Table S1. Crystal structure parameters of Cs_3GdCl_6.

Formula	Cs_3GdCl_6
Temperature (K)	293
M_r	768.68
Crystal system	orthorhombic
Space group	*Pbcm*
a (Å)	8.2273 (2)
b (Å)	13.1409 (4)
c (Å)	26.5472(7)
α (deg)	90
β (deg)	90
γ (deg)	90
V (Å^3)	2870.13(14)
Z	8
ρ_{calc} (g cm^{-3})	3.558
F (000)	2648.0
GOF on F^2	1.053
R_1 [$I > 2\sigma(I)$]	0.0324
wR_2 (all data)	0.0835

Table S2. Nominal and actual doping concentrations of Sb^{3+} in Cs_3GdCl_6: x%Sb^{3+} microcrystals (MCs) synthesized with different molar ratios of Sb to Gd in the precursor solution. The nominal Sb^{3+} doping concentration was defined by the molar ratio of Sb to (Gd + Sb) in the precursor solution, and the actual Sb^{3+} doping concentrations were identified by inductively coupled plasma-atomic emission spectroscopy (ICP-AES) .

Sample	Nominal	Actual
	Sb^{3+} / mol%	Sb^{3+} / mol%
1	0	0
2	0.1	0.1
3	0.5	0.5
4	0.9	1.0
5	1.0	1.2
6	1.5	1.7
7	3.0	3.3
8	5.0	3.4

Table S3. Photoluminescence (PL) parameters of Cs_3GdCl_6: x%Sb^{3+} MCs with different Sb^{3+} concentrations upon ultraviolet (UV) excitation at 330 nm: PL lifetime (τ), PL quantum yield (QY), absorption efficiency (AE), and external quantum efficiency (EQE). The PL lifetimes were determined by single-exponential fitting to the PL decay curves of the MCs.

Sb^{3+} / mol%	τ / μs	PLQY / %	AE / %	EQE / %
0.1	3.15	52.0	43.7	42.1
0.5	2.98	71.7	60.3	58.1
1.0	2.96	96.3	81.0	78.1
1.2	3.10	85.4	71.8	69.2
1.7	2.82	72.2	60.7	58.5
3.3	2.89	60.0	57.5	48.6
3.4	2.78	57.1	55.0	46.3

Table S4. Full-width at half maximum (FWHM) and PL lifetime (τ) of Cs_3GdCl_6: 1.0%Sb^{3+} MCs measured at different temperatures under UV excitation at 330 nm.

T / K	FWHM / meV	τ / μs
80	384	3.39
100	390	3.33
120	397	3.29
140	408	3.15
160	417	2.98
180	427	2.78
200	441	2.69
220	453	2.67
240	468	2.66
260	481	2.62
280	495	2.59
300	510	2.33

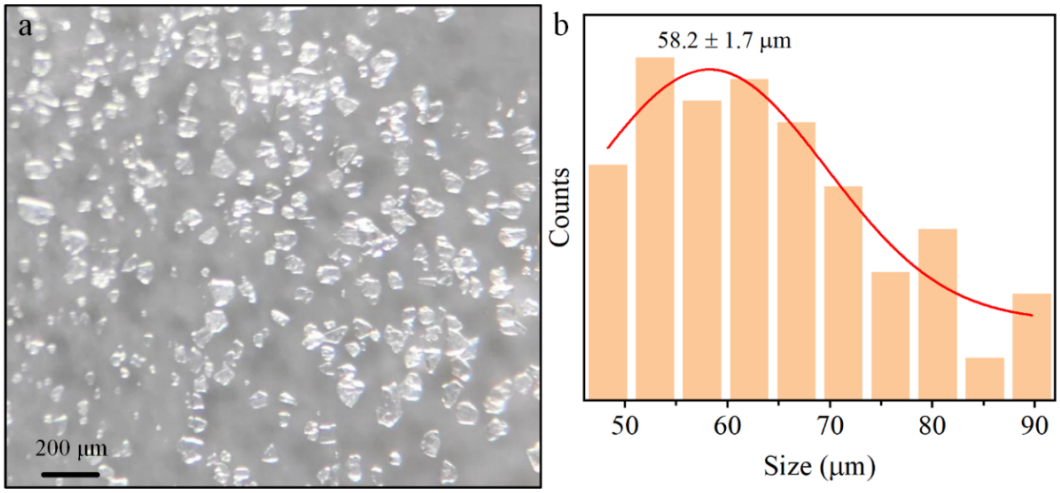

Figure S1. (a) Optical image under ambient light and (b) histogram of size distribution for Cs_3GdCl_6: 1.0%Sb^{3+} MCs. The size distribution was obtained by randomly calculating 200 particles in the optical image.

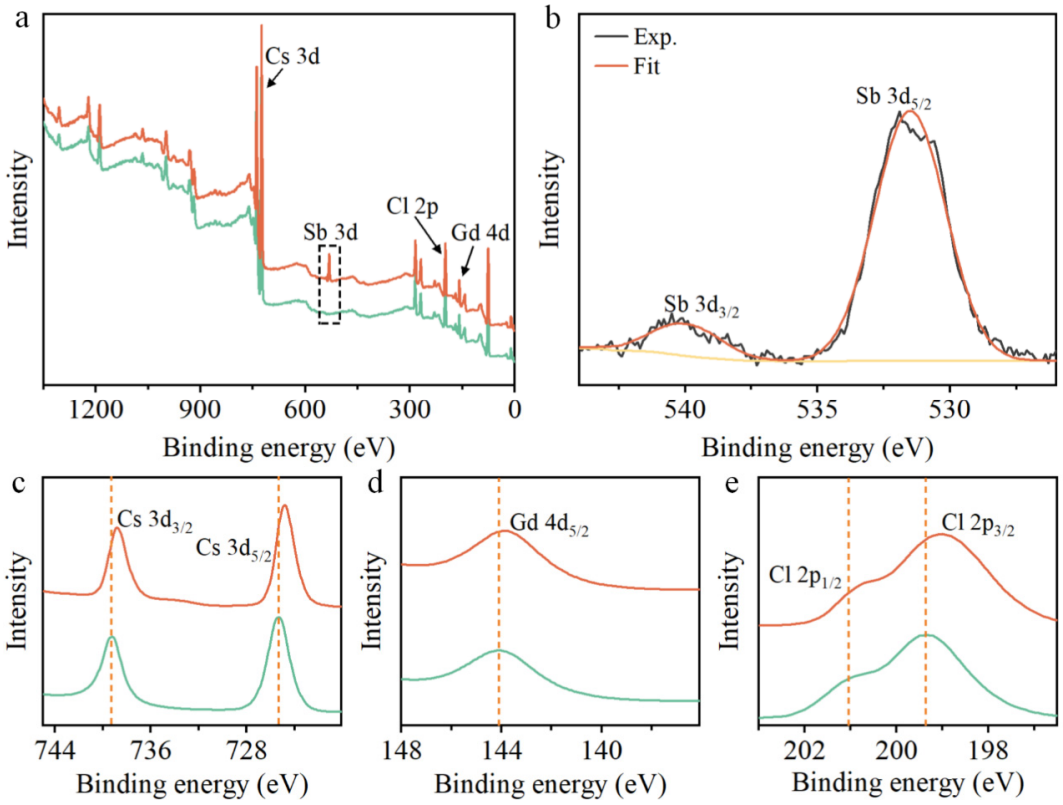

Figure S2. (a) X-ray photoelectron spectra (XPS) of Cs_3GdCl_6 (green) and Cs_3GdCl_6: 1.0%Sb^{3+} (orange) MCs. The spectra are shown over the energy regions typical for (b) Sb 3d, (c) Cs 3d, (d) Gd 4d, and (e) Cl 2p peaks. The peaks at the binding energies of 531.2 and 540.9 eV, 738.2 and 724.2 eV, 144.0 eV, 200.3 and 198.5 eV can be assigned to the Sb^{3+} 3d, Cs^{+} 3d, Gd^{3+} 4d, and Cl^{-} 2p signals, respectively. The Cl 2p and Gd 4d peaks in Sb^{3+}-doped MCs shifted towards lower energies relative to those in the undoped MCs, due to the change in the electron cloud density around $[GdCl_6]^{3-}$ induced by the substitution of Sb^{3+} at the octahedral Gd^{3+} site.

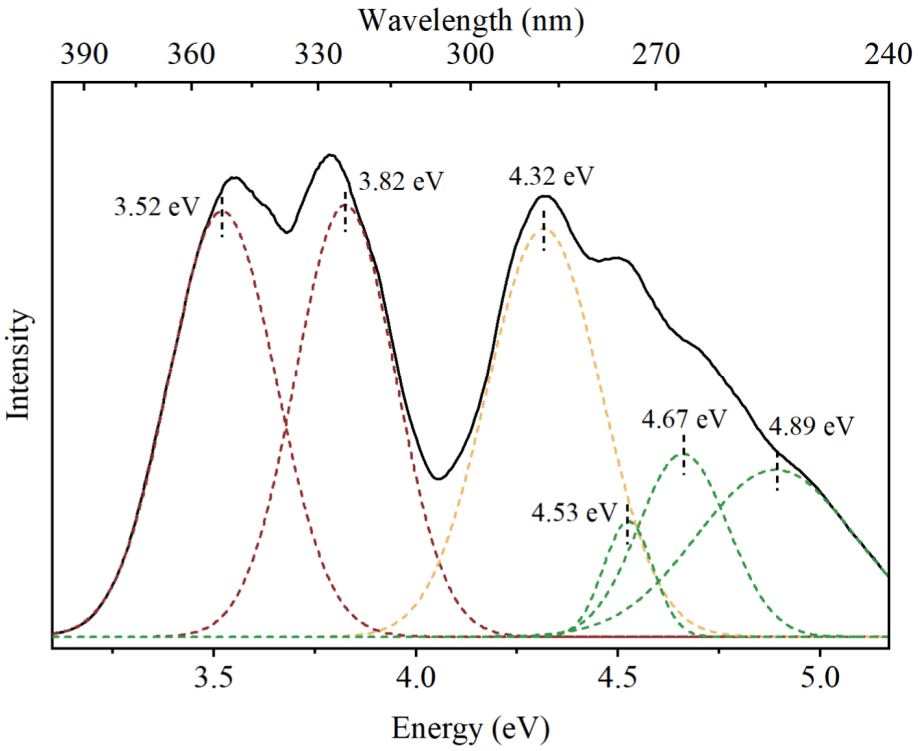

Figure S3. PL excitation spectrum (λ_{em} = 540 nm) of Cs_3GdCl_6: 1.0%Sb^{3+} MCs and the corresponding Gaussian fit. The excitation spectrum was deconvoluted into six bands centered at 4.89 eV (248 nm), 4.67 eV (263 nm), 4.53 eV (275 nm), 4.32 eV (285 nm), 3.82 eV (330 nm), and 3.52 eV (350 nm), respectively. The asymmetric doublet absorption bands at 350 and 330 nm (A band), singlet absorption band at 285 nm (B band), and asymmetric triplet absorption bands at 248, 263, and 275 nm (C band) can be assigned to the spin-orbital allowed $^1S_0 \rightarrow {}^3P_1$, vibration-induced $^1S_0 \rightarrow {}^3P_2$, and dipole-allowed $^1S_0 \rightarrow {}^1P_1$ transitions of Sb^{3+}, respectively.

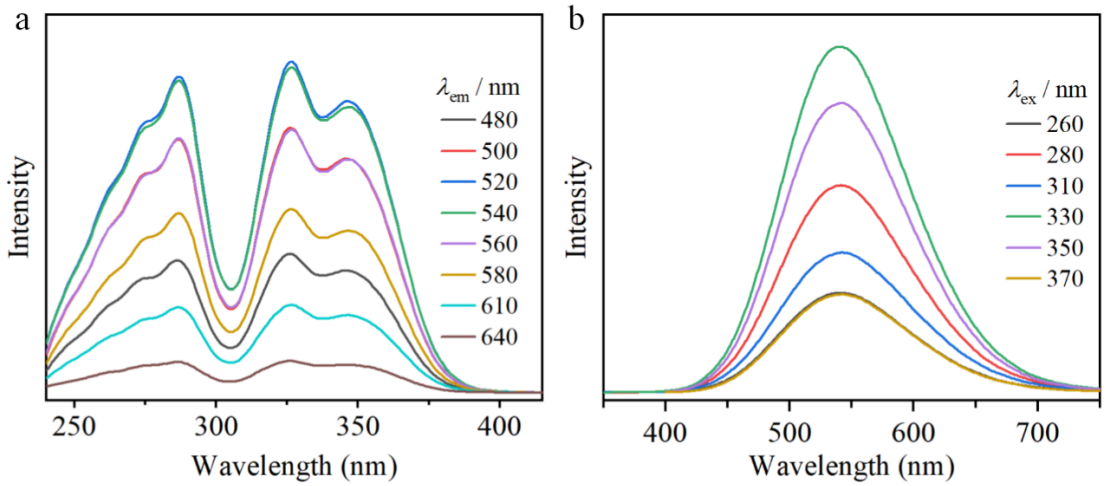

Figure S4. (a) PL excitation spectra of Cs_3GdCl_6: 1.0%Sb^{3+} MCs by monitoring the Sb^{3+} emission at different wavelengths. (b) PL emission spectra of Cs_3GdCl_6: 1.0%Sb^{3+} MCs under excitation at different wavelengths. The excitation and emission patterns were nearly identical, confirming the single luminescent center of Sb^{3+} in Cs_3GdCl_6: 1.0%Sb^{3+} MCs.

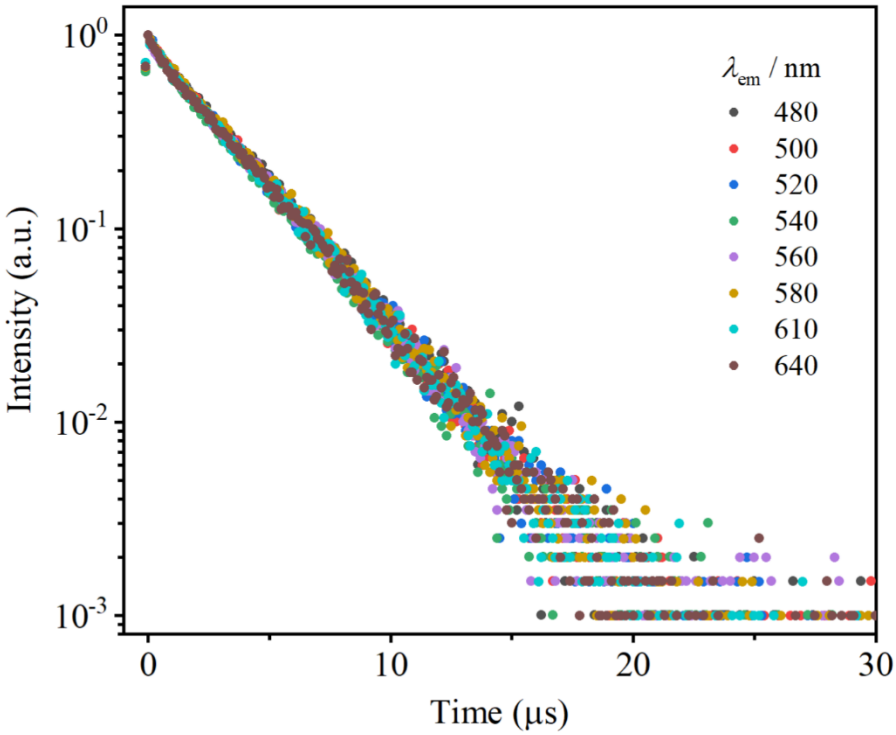

Figure S5. PL decay curves of Cs_3GdCl_6: 1.0%Sb^{3+} MCs by monitoring the Sb^{3+} emission at different wavelengths under UV excitation at 330 nm.

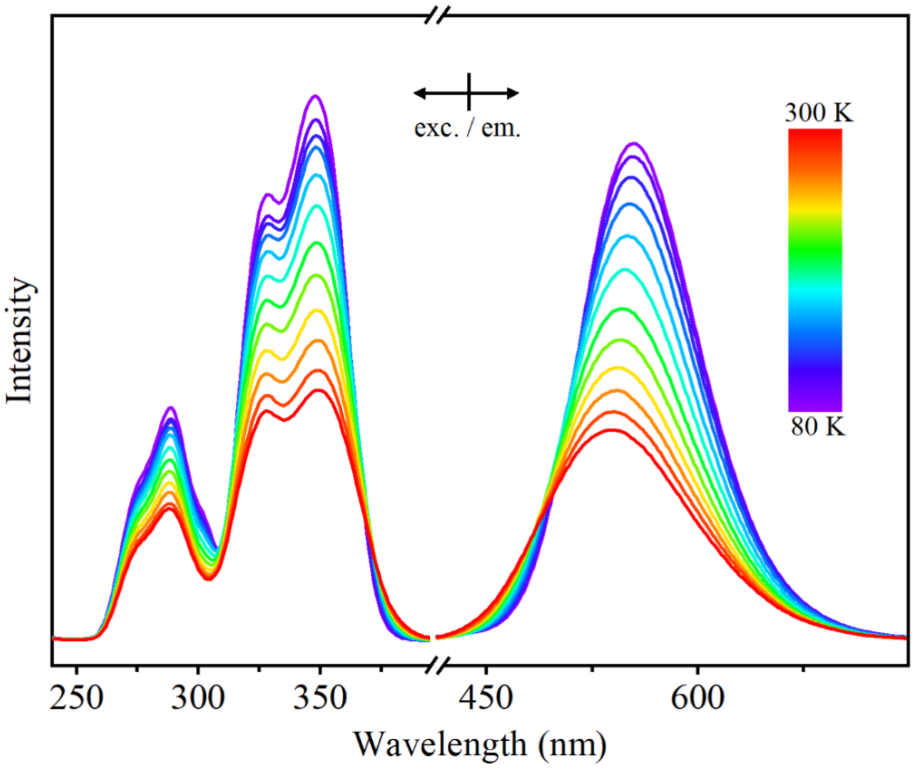

Figure S6. Temperature-dependent PL excitation (left, λ_{em} = 540 nm) and emission spectra (right, λ_{ex} = 330 nm) of Cs_3GdCl_6: 1.0%Sb^{3+} MCs in the temperature range 80–300 K.

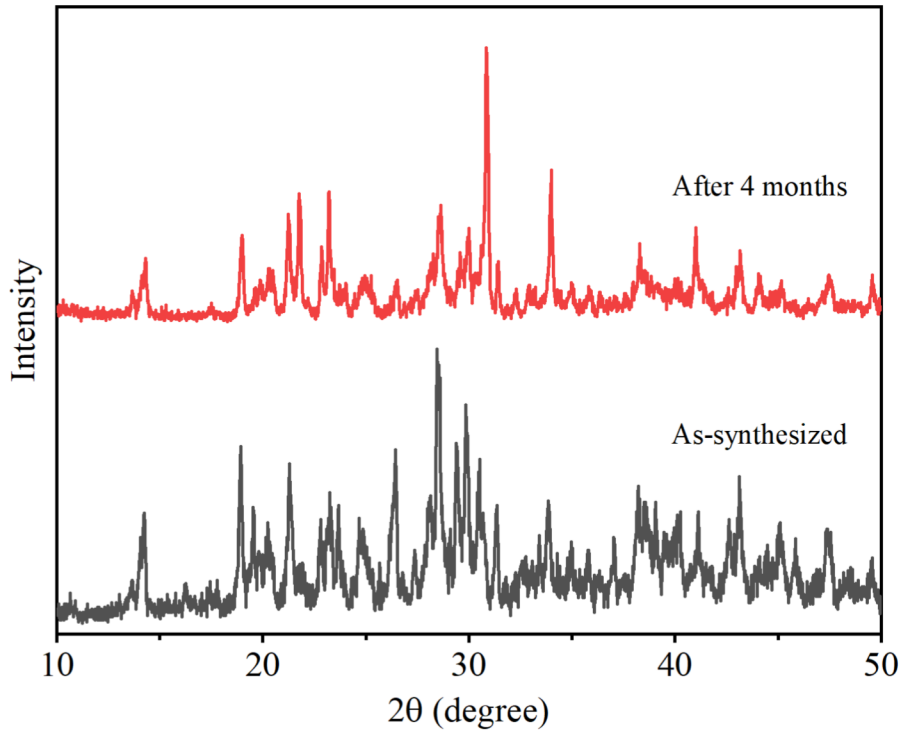

Figure S7. Powder XRD patterns of Cs_3GdCl_6: 1.0%Sb^{3+} MCs before and after their storage in dry air (humidity: 30%) for 4 months. All the diffraction peaks of the MCs can be well indexed into orthorhombic Cs_3GdCl_6.

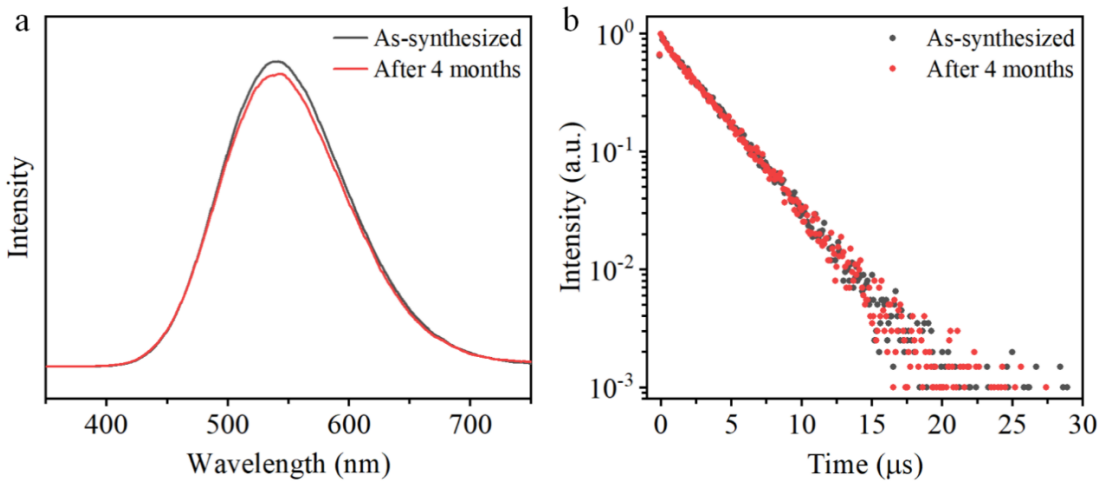

Figure S8. (a) PL emission spectra (λ_{ex} = 330 nm) and (b) PL lifetime (λ_{em} = 540 nm) of Cs_3GdCl_6: 1.0%Sb^{3+} MCs before and after their storage in dry air (humidity: 30%) for 4 months. The PL pattern and PL lifetime of the MCs remained nearly unchanged, indicating good stability of the MCs in dry air.

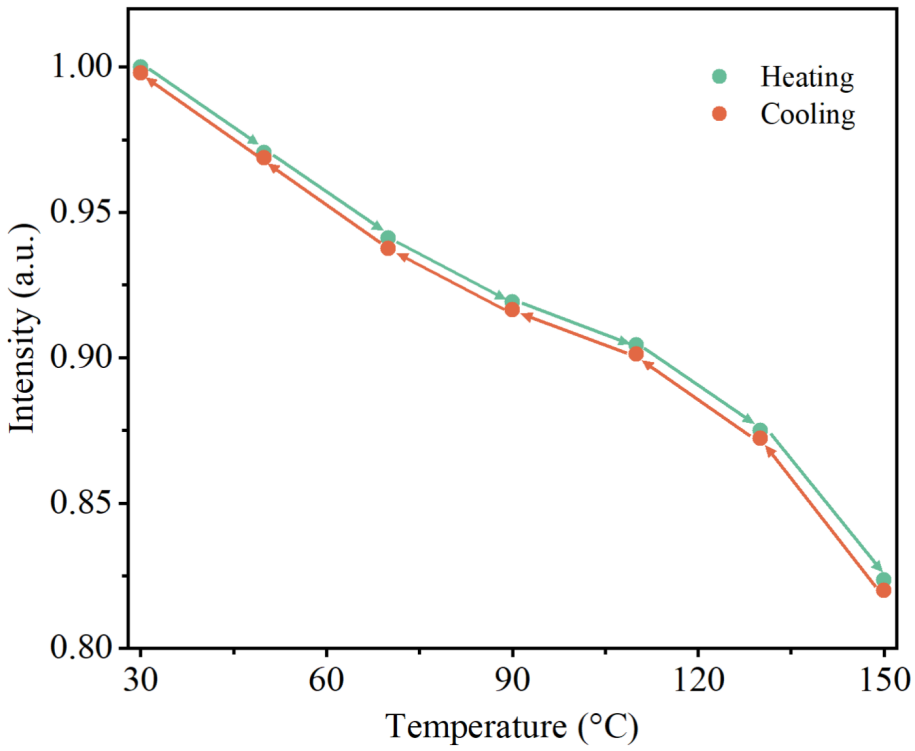

Figure S9. Integrated PL intensities of Cs_3GdCl_6: 1.0%Sb^{3+} MCs as a function of temperature during a heating and cooling cycle between 30 and 150 ºC.

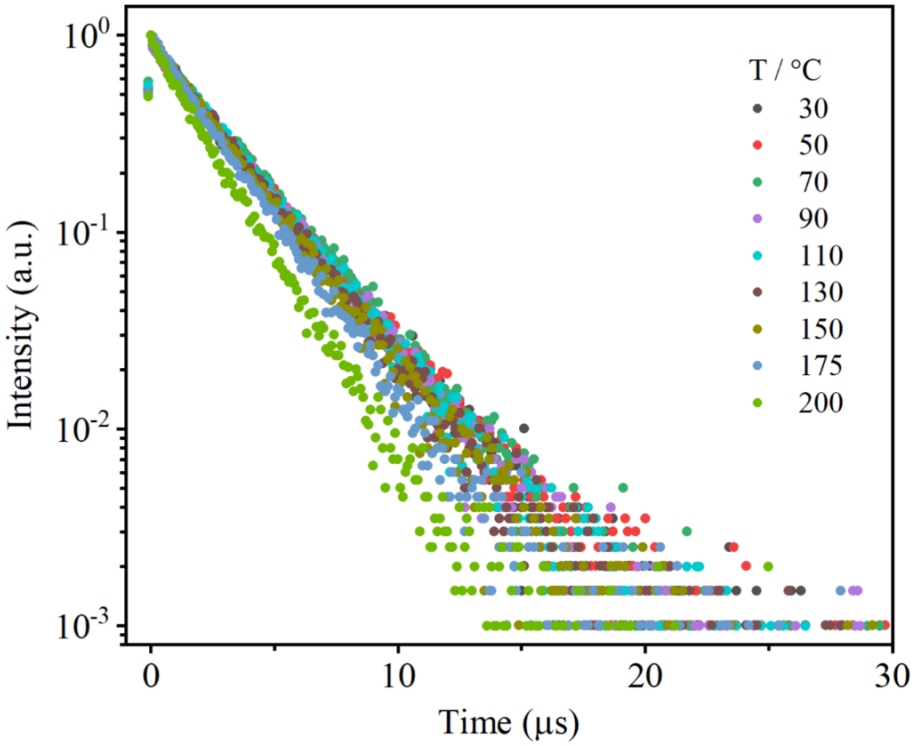

Figure S10. Temperature-dependent (30–200 °C) PL decay curves of Cs_3GdCl_6: 1.0%Sb^{3+} MCs by monitoring the Sb^{3+} emission at 540 nm, showing a gradual decrease in PL lifetime of Sb^{3+} from 2.36 μs to 1.76 μs with the temperature rise from 30 °C to 200 °C, due to the accelerated nonradiative relaxation of Sb^{3+} at higher temperatures.

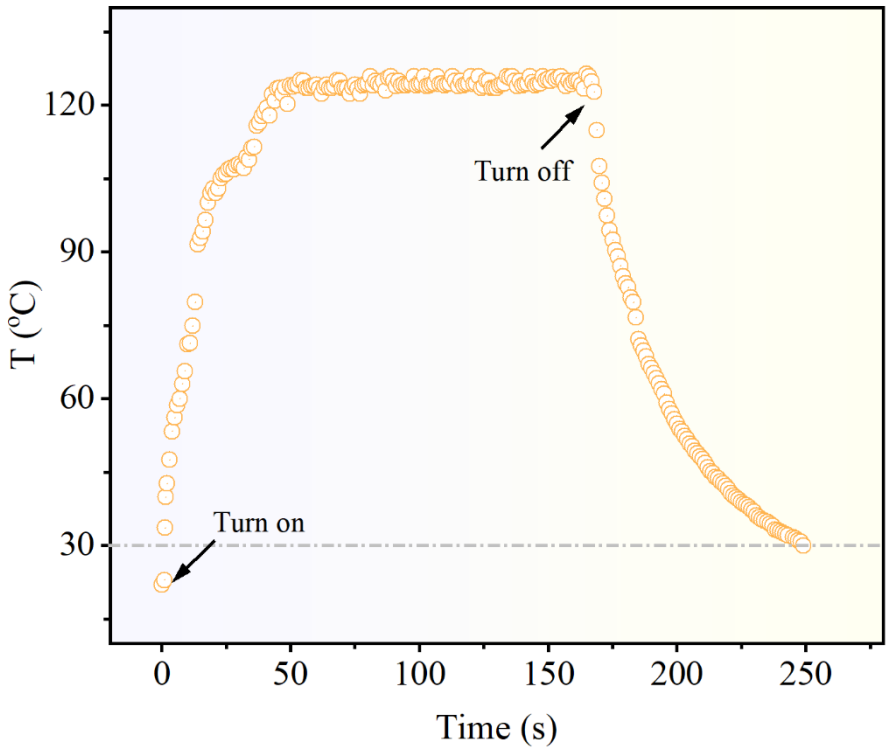

Figure S11. Core temperature variation of the WLED device based on Cs_3GdCl_6: 1.0%Sb^{3+} MCs. The core temperature of the device can be reduced quickly to room temperature within 82 s after switching off the current, manifesting an outstanding thermal diffusion property of the device.